Investigations on Thermal Distribution and Average Power Handling Capability of Substrate-Integrated Waveguide (SIW)

[#]Yumei Chang[1], Wenquan Che[1], Liming Gu[1], Li Li[1]
[1] Department of Communication Engineering, Nanjing University of Science and Technology
210094, Nanjing, China
Email: yeeren_che@yahoo.com.cn

1. Introduction

Taking the advantages of rectangular waveguide (RW) and microstrip, the substrate-integrated waveguide(SIW) has found wide applications in microwave engineering [1]. For highly integrated microwave systems, especially in case of high power, average power handling capability (APHC) is an important issue to consider, which is critically required in practical engineering applications.

As the microwave energy propagates along the waveguides, part of it would be dissipated in the way of Joule heat, which is mainly contributed by Ohmic conductor loss and dielectric loss of the waveguides. In this paper, the APHC of SIW is numerically investigated, which is based on the improved formula of Ohmic loss proposed by Che etc [2]. Factors which may affect the attenuation loss of SIW are also studied. Some important conclusions are given, which may provide useful guidance for the engineering application of SIW structure, especially in case of high power.

2. Attenuation Loss and Heat Transfer in SIW

The schematic structure of SIW is shown in Fig.1 (a), which is an artificial waveguide constructed into a dielectric substrate with dielectric constant ε_r and height h, a' is the width of SIW, while R and W are the cylinder radius and the spacing distance between two adjacent cylinders. To investigate the thermal distribution in the SIW, we will firstly discuss the losses in the SIW, including dielectric loss and conductor loss.

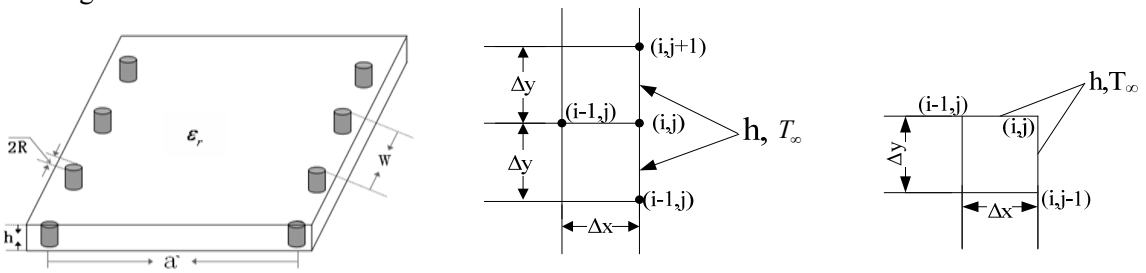

(a) (b) (c)

Fig 1(a) basic structure of SIW; (b) boundaries at the border of SIW; (c) boundaries at the corner of SIW

2.1 Attenuation Loss of SIW

The different loss mechanisms in the SIW by neglecting the radiation loss can be quantified by dividing the total power attenuation constant α per unit length (NP/m) into its Ohmic and dielectric components, named as α_c and α_d, respectively.

As we know, SIW can be analyzed as an equivalent rectangular waveguide; the formula of conductor loss in SIW was derived from the conductor loss of conventional RW [2] and given below

$$\alpha_c = \left[\left(\eta_{sc}\left[\left(\cos^2\frac{\pi a'}{a}\right)\left(\frac{W}{2\pi R}\right)h + \frac{a}{2}\left(\frac{\beta}{k_c}\right)^2 + \left(a' - \frac{a}{2}\right)\right]\right) \Big/ \left(\frac{ah}{2}\left(\frac{\beta}{k_c}\right)^2 \eta_h\right)\right](Np/m) \qquad (1)$$

Where $\eta_{sc} = 1/(\sigma\delta_S)$ is the surface resistance of the solid wall and $\delta_s = 1/\sqrt{\pi f \mu\sigma}$ is the skin depth of the copper. β is the propagation constant in SIW, while k_c is the cut-off wave number of TE_{10} mode in RW, equal to π/a, and the dielectric loss coefficient is $\alpha = \delta_t k^2 / 2\beta$, same as RW.

2.2 Heat Transfer Equation in SIW

The electromagnetic energy dissipated in the transmission lines will be treated as the only source of heating, which lead to the temperature rising. Meanwhile, the heat diffuses to the outside of the lines through radiation and convection.

The equation for the temperature T describing heat conduction in a material is as follows [3]:

$$\rho C\left[\partial T / \partial t + \vec{v} \cdot \nabla T\right] = \nabla \cdot \left[k \nabla T\right] + \left\langle P \right\rangle + q \tag{2}$$

Where $\vec{v}$ is the velocity of the body, which is set to be zero in this work, ρ C and k are the mass density, the specific heat density and the thermal conductivity respectively. Furthermore, q is the heat input per unit volume and per unit time, and the term <P> (W/m^3) indicates the time-averaged heat power absorption density, which is mainly originated from the attenuation loss.

Additionally, boundary conditions should be considered during the analysis, including the heat convection and radiation at the borders of the structures, which are expressed by Eq. (3) ~ (4) [4].

$$q_c = h_c A\left(T_W - T_\infty\right) \tag{3}$$

$$q_r = \xi\sigma A\left(T_W^4 - T_\infty^4\right) \tag{4}$$

Where q_c is the heat loss from convection, and A is the area of the convecting surface, h_c is the heat transfer coefficient between the structure and the air. The constant σ is equal to 5.67×10^{-8} W/m^2K^4, and ξ is the emissivity of the radiating surface, where ξ is the emissivity of copper cladding equal to 0.65. Besides, the initial temperature of the device is assumed to be 20℃, similar to the ambient temperature.

3. Numerical Analysis of APHC in SIW

As the metallic cladding usually has a much higher melting point than the substrate, the heating distortion temperature of the substrate is largely responsible for the APHC limitation. In order to assess the temperature distribution inside the substrate layer, the FDTD method is used to compute the steady-state fields [5], consequently, the dissipated power deposition and the heating patterns in the substrates are determined. Rewriting (2) in its discretized form of two-dimensional case, we can get the following equation,

$$\begin{aligned} T^{n+1}(i,j) = \tau\cdot\Delta t\Big[&\left(T^n(i+1,j) + T^n(i-1,j)/\Delta x^2 + \left(T^n(i,j+1) + T^n(i,j-1)\right)/\Delta y^2\right) \\ &+ P_l(i,j)/k\Big] + \left[1 - \left(2\tau\cdot\Delta t\right)/\Delta x^2 - 2\tau\cdot\Delta t/\Delta y^2\right] T^n(i,j) \end{aligned} \tag{5}$$

Where i and j denote the location of the node, $\triangle x$, $\triangle y$ and $\triangle t$ are the discretization steps along the x, y and t axes, respectively. As for the dissipated power, the temperature nodes are located at the centre of each FDTD cell. But for the nodes at the borders and the exterior corners with convection boundary shown in Fig.1 (b) ~ (c), the explicit nodal equations are expressed as (6) and (7) [4].

$$\begin{aligned} T^{n+1}(i,j) = \tau\cdot\Delta t\Big[&\left(2T^n(i-1,j)\right)/\Delta x^2 + \left(T^n(i,j+1) + T^n(i,j-1)\right)/\Delta y^2 - \left(2\cdot h\Delta x\cdot T_\infty^n\right. \\ &\left./\left(k\cdot\Delta y^2\right)\right) + \left(P_l(i,j)\right)/k\Big] + \left[1 - \left(2\tau\cdot\Delta t\right)/\left(1/\Delta x^2 - 1/\Delta y^2 - h/k/\Delta x\right)\right] T^n(i,j) \end{aligned} \tag{6}$$

$$\begin{aligned} T^{n+1}(i,j) = \tau\cdot\Delta t\Big[&\left(2T^n(i-1,j)\right)/\Delta x^2 + \left(2T^n(i,j-1)/\Delta y^2\right) - \left(2\cdot h\Delta x T_\infty^n/\left(k\cdot\Delta y^2\right)\right) \\ &+ P_l(i,j)/k\Big] + \left[1 - \left(2\tau\cdot\Delta t\right)/\left(1/\Delta x^2 - 1/-h\Delta x/\left(k\Delta y^2\right) - h\Delta y/\left(k\Delta x^2\right)\right)\right] T^n(i,j) \end{aligned} \tag{7}$$

The stability criterion of (5) is given by (8),

$$\Delta t \le \rho C/\left(2k\right)\left(1/\Delta x^2 + 1/\Delta y^2\right)^{-1} \tag{8}$$

It is generally less restricted than the classical stability condition used for the electromagnetic fields in FDTD solution [6].

3.1 APHC of SIW in cases of different operating frequency bands

Three SIW sections, operating at Ku-band, K-band and Ka-band respectively, are investigated. Their parameters and numerical results are listed in Table 1.

Table 1 Three SIW sections operating at different frequency bands (Rogers 5880)

SIW structure	Frequency (f0)	a' (mm)	a (mm)	W (mm)	R (mm)	ε_r	tanδ	α_c (Np/m)	α_d (Np/m)	APHC (W)
Case 1	Ku-Band (15GHz)	10.3	10.1	0.3	0.1	2.2	0.0009	0.3649	0.2814	354
Case 2	K-Band (24GHz)	6.2	6.0	0.3	0.1	2.2	0.0009	0.4706	0.4706	326
Case 3	Ka-Band (33GHz)	4.7	4.6	0.3	0.1	2.2	0.0009	0.5543	0.6176	259

Fig.2 (a) shows the comparison of the total attenuation constants and the APHC in three frequency bands, f_0 is the central frequency of each band. Obviously, the attenuation increases with the operation frequency and the APHC of SIW decreases with the operation frequency. Therefore the average power handling capacity of SIW depends on much on the frequency band, saying, the higher the frequency band, the lower the APHC.

3.2 APHC of SIW in cases of different substrate materials

As we know, substrate materials like Polystyrene and Rogers 5880 are commonly used in RF/MW circuits. Therefore, the APHC of SIW constructed into these materials will be investigated, whose electrical and thermal property parameters are listed in Table 2.

Table 2 Properties of different substrate materials and the numerical results (K-Band)

Substrate Material	ε_r	tanδ	T = $k/\rho C$ (20℃)(m^2/s)	Heat Distortion Temperature(℃)	α_c (Np/m)	α_d (Np/m)	APHC(W)
Polystyrene	2.53	4.7e-4	9.64e-8	100	0.4958	0.2484	25
Rogers 5880	2.2	9.0e-4	1.16e-7	260	0.4706	0.4706	326

Fig.2 (b) illustrates the comparison of the total attenuation loss for the two substrate materials, obviously, the SIW structure constructed in Rogers 5880 has better performance in terms of APHC (326W) than that of Polystyrene (25W) at the operating frequency of 24GHz.However, it can be also seen from the Fig.2 (b) that the attenuation loss of Rogers 5880 is larger than the Polystyrene.

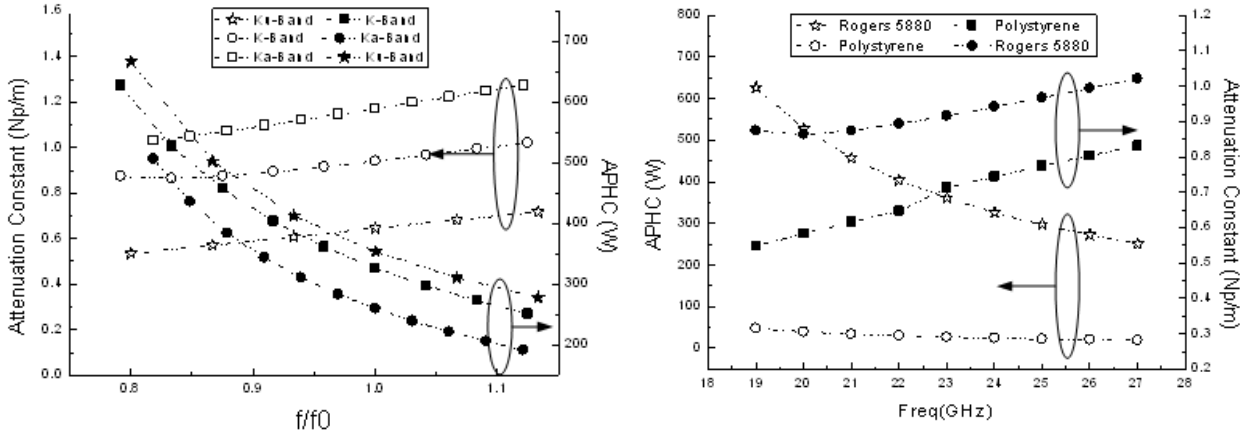

(a) Different frequency bands (b) different substrate materials

Fig. 2Attenuation constants and APHC of SIW at different frequency bands and with different substrate materials

One reason for above results can be explained from the heat distortion temperature of the materials. From Table 2, the heat distortion temperature of Polystyrene is lower than that of Rogers 5880, which means that Polystyrene has lower thermal endurance ability.

Another reason can be explained from the definition of thermal diffusivity τ, saying, the larger the value of τ, the faster heat diffusion through the material. A high value of τ could result either from a high value of thermal conductivity (indicating a rapid energy-transfer rate), or from a low value of the thermal capacity ρC. A low value of the heat capacity would mean that less energy moving through the material would be absorbed and help to raise the temperature of the material; thus more energy would be available for further transfer. In this way, all of these facilitate the thermal dispassion and thus improve the heat endurance of the material.

4. Discussions and Conclusions

The thermal distribution of several SIW structures in different frequency bands and different dielectric substrates are investigated, all the numerical calculations are carried out by FDTD method. Some important results can be concluded below on the basis of above analysis.

1) As the operating frequency increases, total loss in SIW becomes larger, and the temperature rises, resulting in lower average power handling capacity (APHC);

2) The temperature generally increases with the attenuation loss, but not linearly. The temperature comparison in SIW of different substrates indicates that, the temperature in SIW is not only related to their attenuation constants, but also to the thermal properties of the substrate materials.

The thermal distribution and average power handling capacity (APHC) of SIW are investigated in this work, which are very important especially for high power applications. The conductor loss and dielectric loss of SIW are introduced firstly, and are regarded as the heat source in the heat-transfer equation for SIW structure. The thermal distributions inside SIW are calculated by FDTD, from which the APHC are extracted by comparing the maximum temperature in SIW with the heat distortion temperature of the substrate material. From the available results, we may note that, the APHC of Rogers 5880 can be up to 326W at 24GHz. In this way, the SIW structures are the good candidates for high-speed and high-frequency applications, especially in the case of high power.

Acknowledgments

The authors are grateful to the financial support of the National Natural Science Foundation of China (60971013) and the National Key Laboratory Foundation of China (9140C5306010904).

References

[1] D.Deslandes, K.Wu, “Integrated microstrip and rectangular waveguide in planar form,” *IEEE Microwave Wireless Component Letter*, vol. 11, no. 2, pp68-70, Feb. 2001

[2] W.Q.Che, C.X.Li, D.P.Wang, L.Xu. “Investigation on the Ohmic conductor Losses in Substrate-Integrated Waveguide and Equivalent Rectangular Waveguide,” *Journal of Electromagnetic Waves and Appl.* vol.21, no.6, pp769-780, 2007

[3] D. G. Jablonski, “Power-handling capabilities of circular dielectric waveguide at millimetre wavelengths,” *IEEE Trans. Microwave Theory Tech*., vol. MTT-33, no.2, pp. 85-89, Feb. 1985.

[4] J.P. Holman, *Heat Transfer*, 5th edition, New York: McGraw-Hill, 1981

[5] Yongxi. Qian, Tatsuo Itoh, *FDTD Analysis and Design of Microwave Circuits and Antennas-Software and Applications*, 1st edition, Tokyo, Japan: Reakuze Inc.1999

[6] Francois Torres, Bernard Jecko, “Completed FDTD analysis of microwave heating process in frequency-dependant and temperature-dependent media,” *IEEE Trans. Microwave Theory and Techniques*, vol.45, no.1, pp108-117, Jan. 1997